1971

An energy solution for vibration characteristics of free thin cylinders

Dale Elmer Leanhardt

Department:

AN ENERGY SOLUTION FOR VIBRATION CHARACTERISTICS OF FREE THIN CYLINDERS

BY

DALE ELMER LEANHARDT, 1947-

A THESIS

Presented to the Faculty of the Graduate School of the

UNIVERSITY OF MISSOURI-ROLLA

In Partial Fulfillment of the Requirements for the Degree

MASTER OF SCIENCE IN ENGINEERING MECHANICS

1971

Approved by

Lloyd M. Cunningham (advisor) D. B. Ogletree

R. D. Roche

ABSTRACT

In this report the flexural vibrations of the walls of free, thin, circular cylinders are considered. Theoretical expressions are developed for the natural frequencies by extending the approximate energy method of Arnold and Warburton to the free-free case. Furthermore, the developed expressions are shown to apply, as special cases, to the fixed-fixed and simply-supported cylinders analyzed by Arnold and Warburton.

The energy solution for free-free cylinders is checked both experimentally using a 3500 pound-force, 5 to 2000 hertz, vibration exciter and numerically using the well documented SABOR IV-DYNAL finite element program. While the derived energy method accounts for any prescribed number of circumferential waves, only the two and three wave cases were selected for experimental and numerical checking. Cylinder geometric parameters investigated are length/radius = 1, 3, 5, 10, 15, and 20; and radius/wall thickness = 30. The experimental natural frequencies deviate by less than eight percent from the corresponding energy method frequencies. Finite element frequency deviations increase with increasing element length and axial half-wave number, m. They are less than nine percent for element-length/radius ≤ 0.625 and $m \leq 5$. The mode shapes obtained with the finite element program are also in agreement with the assumed displacement forms of the energy method.

ACKNOWLEDGEMENTS

The author owes many thanks to his advisor, Dr. Floyd M. Cunningham, for suggesting the topic and for his guidance and assistance throughout the preparation of this thesis. Special thanks are due Dr. Frank McClarnon and Mr. Bob Scheller of the McDonnell-Douglas Automation Company, St. Louis, Missouri, for their excellent help with the finite element numerical work. Appreciation is also extended to the National Science Foundation for extending to the author a NSF Fellowship which supported in part the work of this thesis.

He is also thankful to Mrs. Judy Hausman for typing the manuscript.

TABLE OF CONTENTS

Page

LIST OF SYMBOLS

a = mean radius of cylinder

h = thickness of the cylinder wall

L = length of the shell

x = axial coordinate

Φ = circumferential coordinate

z = radial coordinate

u, v, w = components of displacement at the middle surface in the axial, tangential, and radial directions

m = number of axial half-waves

n = number of circumferential waves

E = Young's modulus of elasticity

ν = Poisson's ratio

ρ/g = mass density of shell material

ω = circular frequency

ω_o = lowest extensional natural frequency of a ring in plane strain = $[Eg/\rho a^2(1-\nu^2)]^{\frac{1}{2}}$

ω/ω_o = frequency factor

$(...)_{,x}$ = $\partial(...)/\partial x$

$(...)_{,\Phi}$ = $\partial(...)/\partial\Phi$

M_x = bending moment stress resultant

$M_{x\Phi}$ = twisting moment stress resultant

N_x = normal force stress resultant

$N_{x\Phi}$ = in-plane shear force stress resultant

Q_x = transverse shear force stress resultant

T_x = effective tangential shear stress resultant $= N_{x\Phi} - M_{x\Phi}/a$

S_x = effective radial shear stress resultant $= Q_x + (1/a)M_{x\Phi,\Phi}$

X, Y, Z = axes of shell element (Fig. 2)

e_x; e_y = normal strains in X and Y directions for shell element

e_{xy} = shear strain for shell element

ε_1; ε_2 = normal strains in X and Y directions on the middle surface of the shell element

K_1; K_2 = changes of curvature in X and Y directions on the middle surface of the shell element

γ = shear strain on the middle surface of shell element

τ = twist on the middle surface of shell element

T = total kinetic energy of shell

S = total potential energy of shell

t = time

LIST OF FIGURES

LIST OF TABLES

I. INTRODUCTION

The modal vibration characteristics of thin circular cylindrical shells have been studied by many investigators. However, in spite of this extensive coverage, there appear to be no results for free-free boundary conditions. Arnold and Warburton (1)*, in their communication with Grinsted, mention that they had examined the free-free case, but had not published results as they did not appear to have much practical value.

Recent innovation in design and manufacturing techniques, however, indicates a need for free-free thin cylinder vibration characteristics. A particular case, familiar to the author, is the case of rotating machinery with structural shell frames, where the control of vibration and noise radiation is desirable. End plates are usually attached to the ends of the shells. Due to the dimensions and tolerances of the shells and end plates, the fit between them is usually rather loose. What boundary conditions apply? Although the clearance between end plate and shell is small, so are the wall displacements due to shell vibrations, even at resonant frequencies. Furthermore, these displacements decrease when higher normal modes are excited. Thus it is reasonable to assume

---

*Numbers in parentheses refer to the list of references at the end of the thesis.

that the end plates provide little restraint at the shell boundaries, and that free-free boundary conditions apply.

A. Objective

It is the objective of this investigation to determine the flexural vibration characteristics of thin-walled circular cylinders with free-free boundary conditions. The following procedures will be used:

1. Theoretical expressions for the natural frequencies will be developed by extending the approximate energy method of Arnold and Warburton to the free-free case.
2. The energy method results will be compared with the results obtained both experimentally using a 5 to 2000 hertz vibration exciter and numerically using the SABOR IV-DYNAL finite element program.

B. Review of Literature

In 1894, Lord Rayleigh (2) derived an approximate expression for the natural vibratory frequencies of cylindrical shells, in which the motion of all cross-sections is similar, based on a separation of the effects of bending and stretching. In 1927, Love (3) investigated more general vibrations of cylinders. His work resulted in a general dynamical theory of shells which included both bending and extensional deformations, but did not include frequency equations for any specified end condition. In

1934, Flugge (4) used Love's equations to obtain a cubic frequency equation for a simply-supported cylinder, a result which indicated that there were three frequencies for each modal pattern. A more detailed investigation of simply-supported cylinders by Arnold and Warburton (5) in 1949 showed that the three frequencies correspond to predominately radial, axial, and tangential vibrations with the predominately radial vibration frequency much lower than the other two. Later, Arnold and Warburton also investigated the natural frequencies of cylinders clamped at both ends, by using a Rayleigh-Ritz approach in which beam functions were used as radial, axial, and tangential displacement functions. Since only one beam function was used for each displacement component, their work was based on a very rudimentary form of the Rayleigh-Ritz method. The present paper extends this method of Arnold and Warburton to the free-free case.

Many other investigators have studied the vibration of thin cylinders. Three approaches seem to exist. An exact method, outlined by Flugge (6) and used by Forsberg (7), establishes the influence of boundary conditions on the modal characteristics of thin cylindrical shells. Another exact method was used in a recent thesis by Sharma (8) in which the differential shell equations were integrated numerically with the aid of a suppression technique. Most recently, investigators have concentrated on simplifying

the analysis of vibrating cylindrical shells by development of a number of approximate energy methods. References for these methods can be found in Weingarton (9). Finally, some investigators such as Gottenberg (10), have conducted detailed experiments on cylindrical shell vibrations.

II. ENERGY SOLUTION

Typical vibration modal forms for a free-free thin cylinder are shown in Fig. 1. The circumferential forms of Fig. 1b are the exact sinusoidal shapes presented by Arnold and Warburton (1) and again by Forsberg (7). Since these forms are independent of end boundary conditions, they are applicable to free-free cylinders. The axial forms of Fig. 1a and the modal arrangement of Fig. 1c are plausible configurations assumed for the free-free cylinder of the present investigation.

The theoretical expressions to be developed pertain to $n \geq 2$ and $m \geq 1$. Forsberg (11) showed that the behaviors of a cylindrical shell in axisymmetric (n=0) and beam-type (n=1) motion can be adequately predicted by considering the cylinder as a ring for n=0 modes and as a compact beam for n=1 modes. Furthermore, he noted that the minimum natural frequency of a cylindrical shell is generally associated with a mode having two or more circumferential waves. Thus, the fact that the following energy solution pertains only to $n \geq 2$ does not limit its importance in any way.

A. Development of Cubic Frequency Equation for Free-Free Cylinders

1. Method of Development

The strain components of a differential element of

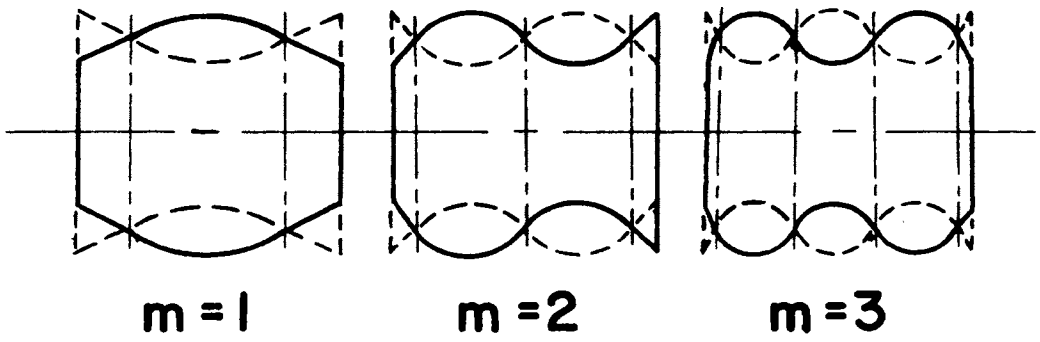

(a) AXIAL MODAL FORMS

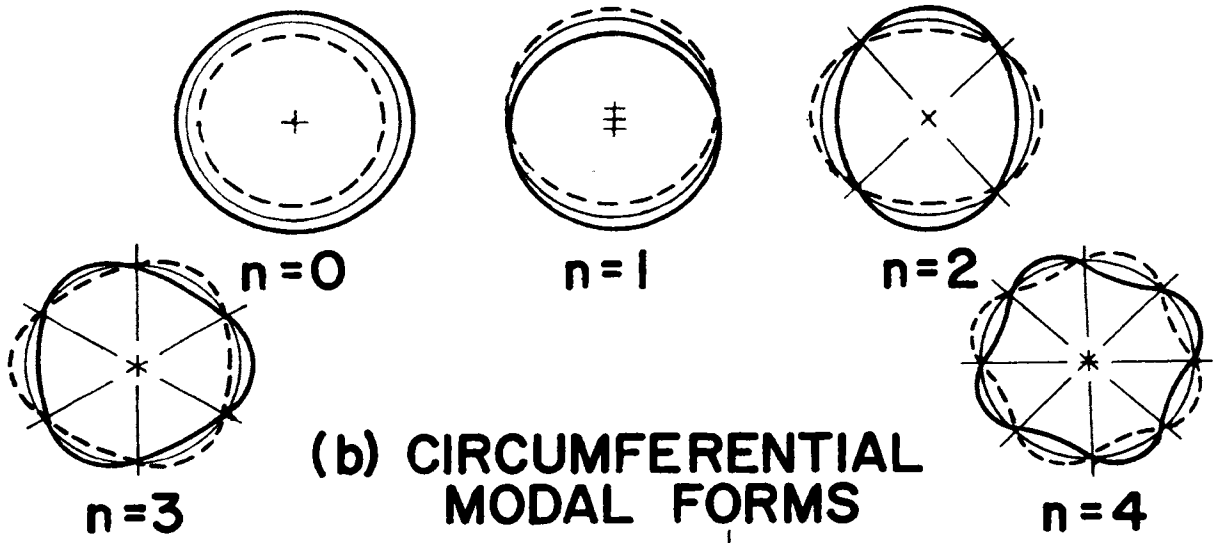

(b) CIRCUMFERENTIAL MODAL FORMS

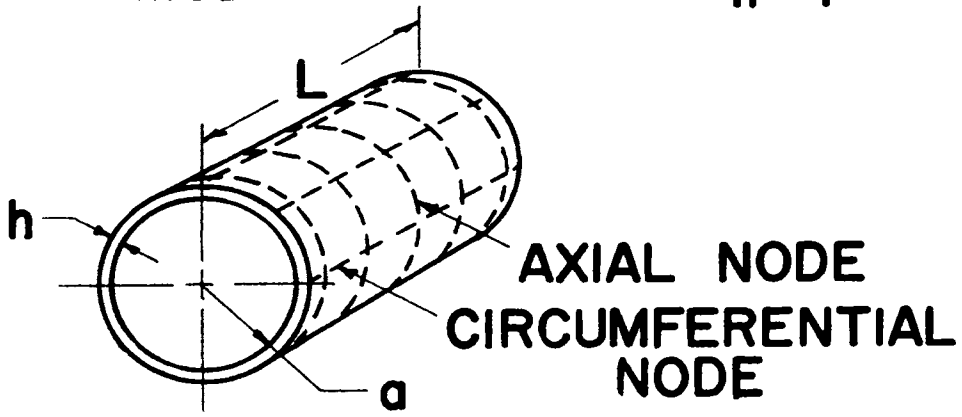

(c) NODAL ARRANGEMENT FOR n = 3, m = 4

Fig. 1. Modal forms

the cylinder are used in the elastic constitutive equations to obtain an expression for strain energy. Using the strain-displacement equations developed by Love (3), strain energy is expressed in terms of the rectangular displacements u, v, and w. Kinetic energy is expressed in terms of $u_{,t}$; $v_{,t}$; and $w_{,t}$. With the assumption that the vibration of free-free cylinders is similar to that of free-free, Bernoulli-Euler beams; suitable expressions are chosen for u, v, and w such that the dependence of radial displacement, w, with the axial coordinate, x, takes the form of a free-free beam.

After the selection of expressions for u, v, and w, equations for strain energy and kinetic energy are derived which lend themselves to analysis by energy principles such as Lagrange's equation. Applying Lagrange's equation three times, once for each of the three independent displacements u, v, and w, three equations of motion are obtained. By solving the equations of motion and eliminating the arbitrary amplitude constants, a cubic frequency equation is obtained. The roots of this equation give three frequencies associated with: one, a predominately radial mode; two, a predominately tangential mode; and three, a predominately axial mode.

2. Formulation

The triple integrals of Eq. (1) for linear-elastic strain energy and of Eq. (2) for kinetic energy, are given by Arnold and Warburton (1) for the differential shell element of Fig. 2.

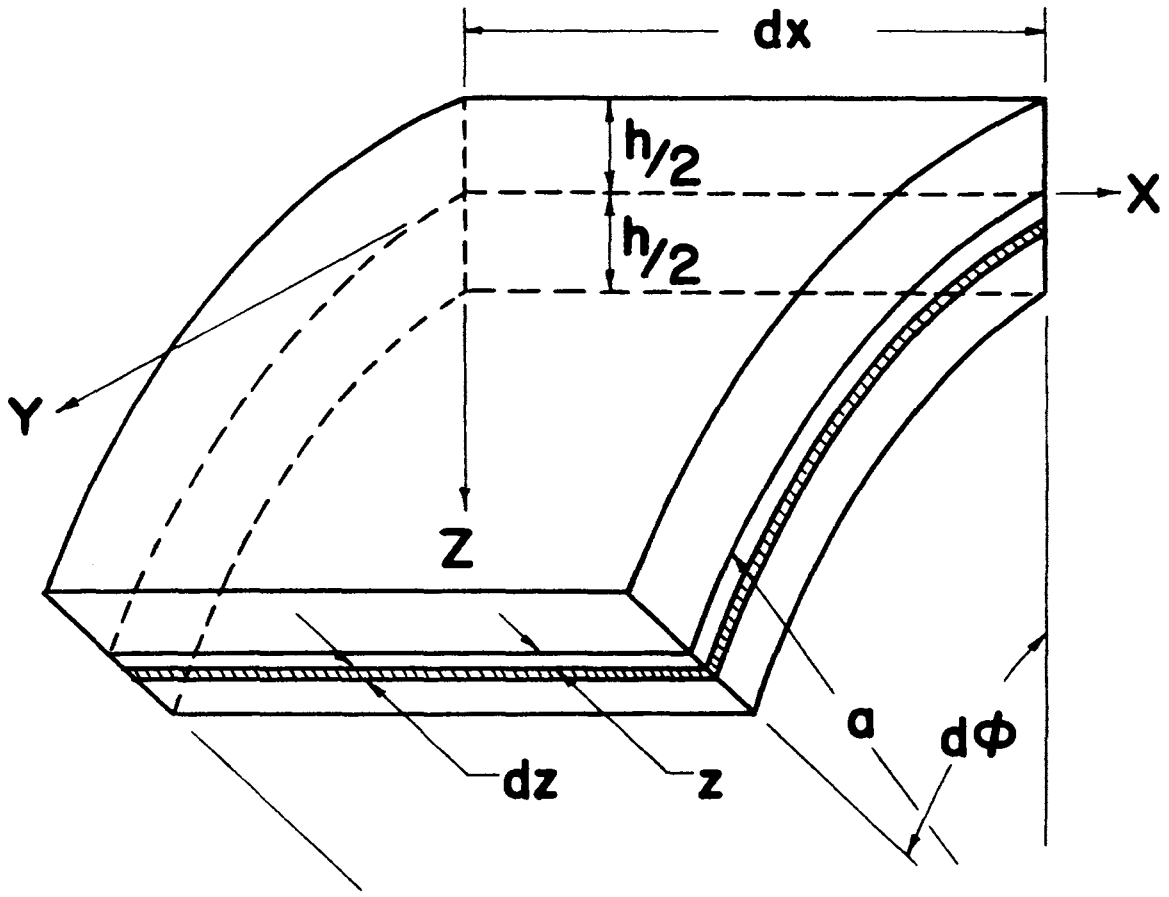

Fig. 2. Differential shell element

$$S = \frac{E}{2(1-\nu^2)} \int_0^{2\pi} \int_{-L/2}^{L/2} \int_{-h/2}^{h/2} \{e_x^2 + e_y^2 + 2\nu e_x e_y + \tfrac{1}{2}(1-\nu)\, e_{xy}^2\}\ a\, d\Phi\, dx\, dz \qquad (1)$$

$$T = \frac{\rho}{2g} \int_0^{2\pi} \int_{-L/2}^{L/2} \int_{-h/2}^{h/2} \{(u_{,t})^2 + (v_{,t})^2 + (w_{,t})^2\}\ a\, d\Phi\, dx\, dz \qquad (2)$$

Eqs. (3) were derived by Love (3) and represent the strains at a distance z from the middle surface of the deformed shell.

$$e_x = \varepsilon_1 - zK_1 \quad e_y = \varepsilon_2 - zK_2 \quad e_{xy} = \gamma - 2z\tau \qquad (3a\text{-}c)$$

$$\varepsilon_1 = u_{,x} \quad \varepsilon_2 = \frac{1}{a}(v_{,\Phi} - w) \quad \gamma = v_{,x} + \frac{1}{a} u_{,\Phi} \qquad (3d\text{-}f)$$

$$K_1 = w_{,xx} \quad K_2 = \frac{1}{a^2}(w_{,\Phi\Phi} + v_{,\Phi}) \quad \tau = \frac{1}{a}(w_{,x\Phi} + v_{,x}) \qquad (3g\text{-}i)$$

In deriving the above equations the basic assumptions of small displacement theory and thin shell theory were used such that higher order terms could be eliminated as discussed by Love (3) and again by Timoshenko (12).

With the strain energy, kinetic energy and strain displacement Eqs. (1), (2), and (3), the development may proceed. The dependence of radial displacement, w, with axial coordinate, x, is assumed to be of the same form as that of a Bernolli-Euler free-free beam as indicated in Fig. 1a. The dependence of tangential dis-

placement, v, with x is assumed to be of the same form as radial displacement, w, since these two components of motion are directly coupled at each cross section. The dependence of axial displacement, u, with x is assumed to be of the form $w_{,x}$. This assumed displacement for u is reasonable since it gives zero normal strains, $u_{,x}=0$, at the ends of the cylinder and maximum normal strains at all radial motion antinodes. Finally, it should be noted that these assumed displacement forms were chosen in the same manner as that of Arnold and Warburton (1) for fixed-fixed cylinders. The accuracy of the results by Arnold and Warburton, therefore, give good justification for the above choices of dependence of u, v, and w with the axial coordinate, x.

3. Analysis

To simplify the analysis, the origin is taken at the mid-point of the cylinder. Thus, the two possibilities of even and odd number of axial nodes must be considered separately, since they have different displacement functions due to the different conditions of symmetry at the origin. When the number of nodes is even, $w_{,x}=0$ at the origin; and when it is odd, $w=0$.

(a) Even Number of Axial Nodes. The assumed displacement functions are

$$u = U(-\sin\frac{\mu}{a}x - k \sinh\frac{\mu}{a}x) \cos(n\Phi) \qquad (4a)$$

$$v = V(\cos\frac{\mu}{a}x - k\cosh\frac{\mu}{a}x)\sin(n\Phi) \tag{4b}$$

$$w = W(\cos\frac{\mu}{a}x - k\cosh\frac{\mu}{a}x)\cos(n\Phi) \tag{4c}$$

where U, V, and W are functions of time only and

$$k = \frac{\sin\frac{\mu L}{2a}}{\sinh\frac{\mu L}{2a}}$$

The values of μ are given by

$$\tan\frac{\mu L}{2a} = -\tanh\frac{\mu L}{2a}$$

for which the roots are

$$\frac{\mu}{a}L = 1.506\pi,\ \frac{7}{2}\pi,\ \frac{11}{2}\pi,\ \frac{15}{2}\pi,\ \ldots.$$

corresponding to 2, 4, 6, 8,...axial nodes or 1, 3, 5, 7...axial half-waves (m=1, 3, 5, 7...). Substituting Eqs. (4) into Eqs. (3) and then using Eqs. (1) and (2), the strain energy and kinetic energy expressions can be integrated. The steps of integration are presented in Appendix A. The results are

$$S = \frac{\pi EhL}{4a(1-\nu^2)}\{\mu^2\Theta_1U^2 + \beta\mu^4\Theta_1W^2 + \Theta_1\left[(nV-W)^2 + \beta(nV-n^2W)^2\right] + 2\nu\Theta_2\left[-\mu nUV + \mu UW + \beta(\mu^2n^2W^2 - \mu^2nVW)\right] + \tfrac{1}{2}(1-\nu)\Theta_3\left[n^2U^2 + \mu^2V^2 - 2\mu nUV + 4\beta(\mu^2V^2 + \mu^2n^2W^2 - 2\mu^2nVW)\right]\} \tag{5}$$

where $\beta = \frac{h^2}{12a^2}$ and $\Theta_1 = 1 + k^2$

$$\Theta_2 = 1 - k^2 + \frac{2a}{\mu L}\sin\frac{\mu}{a}L$$

$$\Theta_3 = 1 - k^2 - \frac{6a}{\mu L}\sin\frac{\mu}{a}L$$

$$T = \frac{\pi\rho haL}{4g}\left[\Theta_3\dot{U}^2 + \Theta_1(\dot{V}^2 + \dot{W}^2)\right] \tag{6}$$

where $\dot{U}$, $\dot{V}$, and $\dot{W}$ represent the derivatives of U, V, and W with respect to time, t. Applying Lagrange's equation

$$\frac{d}{dt}(T,_{\dot{U}}) - (T,_U) = -S,_U \tag{7}$$

Two similar equations of motion for the degrees of freedom, V and W, can be obtained by applying Lagrange's equation two more times. Substituting U=A cos(ωt), V=B cos(ωt), and W=C cos(ωt) into the three equations of motion and letting $\Delta=\rho(1-\nu^2)\omega^2a^2/Eg$, the following three equations are obtained.

$$\{\mu^2\Theta_1 + \tfrac{1}{2}(1-\nu)n^2\Theta_3 - \Delta\Theta_3\}A - \{\tfrac{1}{2}(1-\nu)\mu n\Theta_3 + \nu\mu n\Theta_2\}B + \{\nu\mu\Theta_2\}C = 0 \tag{8a}$$

$$-\{\nu\mu n\Theta_2 + \tfrac{1}{2}(1-\nu)\Theta_3\mu n\}A + \{n^2\Theta_1 + \tfrac{1}{2}(1-\nu)\mu^2\Theta_3 - \Delta\Theta_1 + \beta[n^2\Theta_1 + 2(1-\nu)\mu^2\Theta_3]\}B - \{n\Theta_1 + \beta[n^3\Theta_1 + \nu\mu^2n\Theta_2 + 2(1-\nu)\mu^2n\Theta_3]\}C = 0 \tag{8b}$$

$$\{\nu\mu\Theta_2\}A - \{n\Theta_1 + \beta[n^3\Theta_1 + \nu\mu^2n\Theta_2 + 2(1-\nu)\mu^2n\Theta_3]\}B + \{\Theta_1 - \Delta\Theta_1 + \beta[\mu^4\Theta_1 + n^4\Theta_1 + 2\nu\mu^2n^2\Theta_2 + 2(1-\nu)\mu^2n^2\Theta_3]\}C = 0 \tag{8c}$$

The above three equations, Eqs. (8), contain four unknowns, the arbitrary amplitude constants A, B, and C, and the desired natural frequency, ω. By combining Eqs. (8), a cubic frequency equation and amplitude ratios are obtained. This reduction process is contained in Appendix B. Results are

$$\Delta^3 - R_2\Delta^2 + R_1\Delta - R_0 = 0 \qquad (9)$$

where $R = 1/(\theta_1^2\theta_3)$

$R_2 = R(J\theta_1\theta_3 + H\theta_1\theta_3 + G\theta_1^2)$

$R_1 = R(GJ\theta_1 + GH\theta_1 - HJ\theta_3 - y_3z_2\theta_3 - y_1x_2\theta_1 - x_3z_1\theta_1)$

$R_0 = R(x_2y_3z_1 - Gy_3z_2 - y_1x_2J - x_3z_1H - x_3y_1z_2 + GHJ)$

$G = \left[\mu^2\theta_1 + \tfrac{1}{2}(1-\nu)n^2\theta_3\right]$

$H = \{n^2\theta_1 + \tfrac{1}{2}(1-\nu)\mu^2\theta_3 + \beta[n^2\theta_1 + 2(1-\nu)\mu^2\theta_3]\}$

$J = \{\theta_1 + \beta[\mu^4\theta_1 + n^4\theta_1 + 2\nu\mu^2n^2\theta_2 + 2(1-\nu)\mu^2n^2\theta_3]\}$

$y_1 = -\left[\nu\mu n\theta_2 + \tfrac{1}{2}(1-\nu)\mu n\theta_3\right]$

$z_1 = \nu\mu\theta_2$

$z_2 = -\{n\theta_1 + \beta[n^3\theta_1 + \nu\mu^2n\theta_2 + 2(1-\nu)\mu^2n\theta_3]\}$

$x_2 = y_1$

$y_3 = z_2$

$x_3 = z_1$

$\Delta = \rho a^2\omega^2(1-\nu^2)/Eg$

(b) Odd Number of Axial Nodes. The assumed displacement functions are

$$u = U(\cos\tfrac{\mu}{a}x + k\cosh\tfrac{\mu}{a}x)\cos(n\Phi) \qquad (10a)$$

$$v = V(\sin\frac{\mu}{a}x + k \sinh\frac{\mu}{a}x) \sin(n\Phi) \tag{10b}$$

$$w = W(\sin\frac{\mu}{a}x + k \sinh\frac{\mu}{a}x) \cos(n\Phi) \tag{10c}$$

where the definitions of U, V, W, and k are the same as before, but the values of μ are given by

$$\tan\frac{\mu L}{2a} = \tanh\frac{\mu L}{2a}$$

for which the roots are

$$\frac{\mu}{a}L = \frac{5}{2}\pi, \frac{9}{2}\pi, \frac{13}{2}\pi, \frac{17}{2}\pi, \ldots.$$

corresponding to 3, 5, 7, 9...axial nodes or 2, 4, 6, 8...axial half-waves (m=2, 4, 6, 8...).

Using the procedures discussed previously for an even number of axial nodes, the same form of cubic equation in ω is obtained provided we redefine the values of Θ as follows:

$$\Theta_1 = 1 + (-1)^{m+1} k^2 \tag{11a}$$

$$\Theta_2 = 1 + (-1)^{m+1} (\frac{2a}{\mu L} \sin\frac{\mu}{a}L - k^2) \tag{11b}$$

$$\Theta_3 = 1 + (-1)^{m}(\frac{6a}{\mu L} \sin\frac{\mu}{a}L + k^2) \tag{11c}$$

where m+1 is the number of axial nodes and m is the number of axial half-waves.

(c) Summary. Using Eqs. (9) and (11) along with Eqs. (12) below,

$$\frac{\mu}{a}L = 1.506\pi \qquad \text{for } m = 1 \tag{12a}$$

$$\frac{\mu}{a}L = (m + 0.5)\pi \qquad \text{for } m \geq 2 \tag{12b}$$

the three frequencies corresponding to predominately radial, axial, and tangential vibration of a free-free thin cylinder may be determined by solving the resulting cubic equation.

B. Application of Frequency Equation to Fixed-Fixed and Simply-Supported Cases

It may be noted that the frequency equations developed by Arnold and Warburton (1) for fixed-fixed and simply-supported thin cylinders are special cases of the frequency equation developed for free-free cylinders. If Eqs. (9) and (12) are left the same, and Eq. (11c) is changed such that

$$\Theta_3 = 1 + (-1)^{m+1}\left(\frac{2a}{\mu L}\sin\frac{\mu}{a}L - k^2\right)$$

the results apply to the case of a fixed-fixed cylinder. If Eq. (9) is left the same and Eqs. (11) and (12) are changed such that $\Theta_1=\Theta_2=\Theta_3=1$ and $\frac{\mu}{a}L=m\pi$, the results now apply to the case of a simply-supported cylinder. Frequencies calculated in this way for the fixed-fixed and simply-supported cases agree exactly with those obtained from the expressions of Arnold and Warburton (1). These expressions were compared with a direct-integration solution by Sharma (8). He reported a maximum error of less than ten percent for cylinders investigated.

III. METHODS OF VERIFICATION

The energy solution of this investigation, presented in Eqs. (9), (11), and (12), was verified both experimentally in the laboratory and numerically with the SABOR IV-DYNAL finite element program. Descriptions of both methods of verification are given in the following paragraphs and Figs. 3, 4, and 5.

A. Experimental

Thin cylinders were mounted in the free-free condition to a 3500 pound-force MB C25HAA vibration exciter by continuous ring contacts at axial nodal locations as shown in Fig. 3. A 0.063-diameter-wire snap ring provided continuous contact around the circumference at the axial nodal locations for the tangential and radial components of motion. In Fig. 4, this snap ring is shown in the groove of the fixture insert. The nodal locations were determined from finite element program output for each normal mode to be investigated. The desired distance between nodal supports was obtained by two adjustments. First the aluminum fixtures could be attached at one-inch intervals to the base plate through a pre-drilled hole pattern. Second, the fixture inserts containing the wire snap ring supports could be located within the fixtures anywhere within the one-inch intervals by means of the four adjusting screws. Thus, any location along the cylinder, within the limits (16-inch maximum) of the base plate, could be obtained

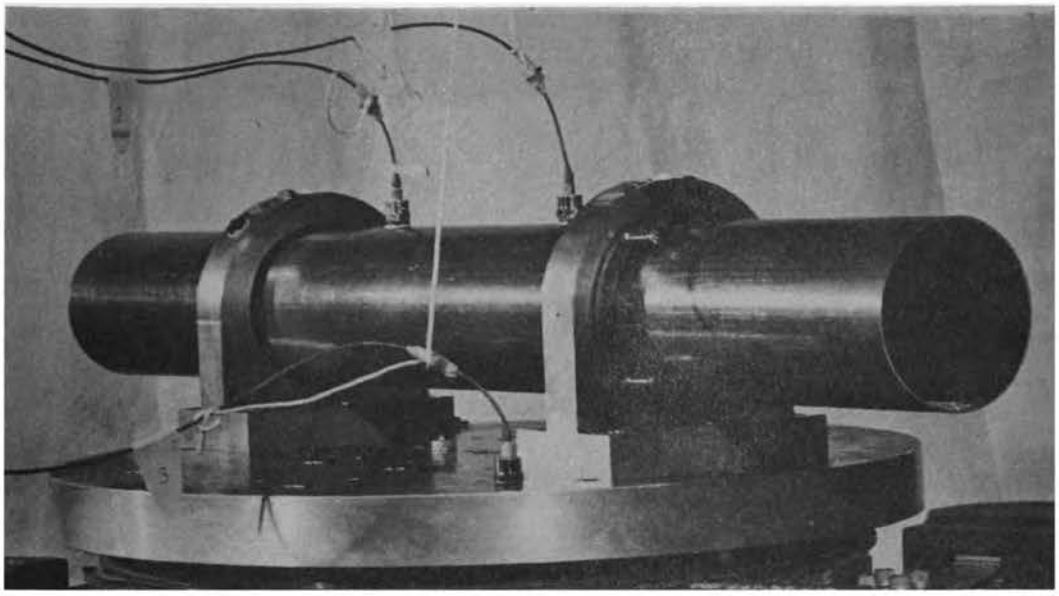

Fig. 3. Free-free cylinder mounted on vibration exciter

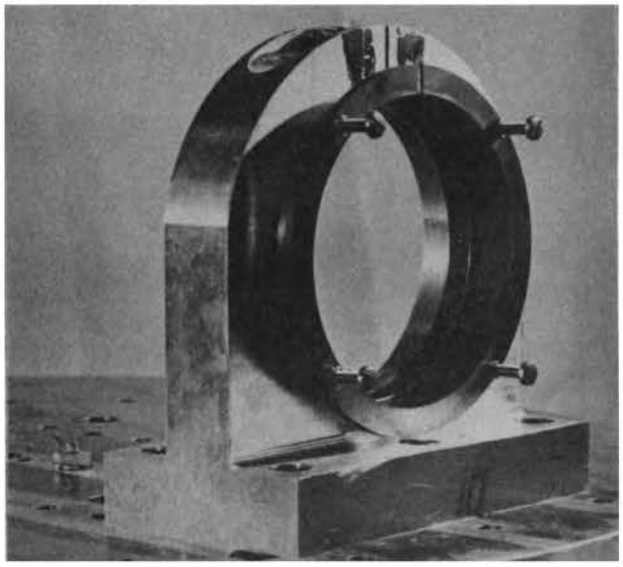

Fig. 4. Test fixture

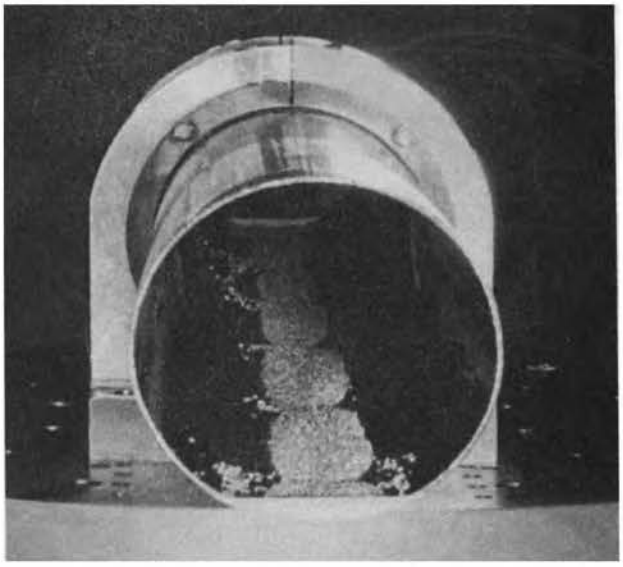

Fig. 5. Sand distribution due to m=5 vibration

in order to support the cylinder at nodal locations.

The shell geometry parameters, circumferential wave numbers, and axial half-wave numbers investigated experimentally are:

$L/a = 20, 15, 10$ and 5

$a/h = 30$

$n = 2$ and 3

$m = 1, 2, 3, 4, 5$

All combinations of the above values for n and m could not be investigated for each L/a ratio due to limitations imposed by the 5-2000 hertz frequency range of the exciter and the 2.0 - 16.0 inch range of the fixture hole pattern. The cylinders were lengths of cold-drawn seamless steel tubing having a 4.0-inch O.D. and a 0.065-inch wall thickness.

A combination of experimental techniques were used to determine particular modal characteristics. Natural frequencies were determined during scanning of the frequency spectrum by watching the 180° phase reversals of two accelerometers mounted on the wall of the cylinder, by noting the maximum g-levels on the g-meters, and by observing the maximum sand activity inside the cylinder. Mode shapes were determined by observing the sand distribution inside the cylinder, as shown in Fig. 5, and by a tracing method using a phonograph cartridge as a vibration pick-up. In the tracing method, the signal from an accelerometer mounted on the base plate was fed to one

plate of a cathode-ray tube and the signal from the vibration pick-up was fed to the other plate. Nodal lines were readily identified by the change in the phase ellipse as the pick-up passed through them.

B. Finite Element

The well documented SABOR IV-DYNAL program of the McDonnell-Douglas Automation Company was also used to verify the energy solution. The program makes use of two existing computer programs, SABOR IV and ICES-DYNAL, which have been integrated by McDonnell to provide natural frequencies and mode shapes of axisymmetric shells. The SABOR IV program generates a stiffness matrix and a consistent mass matrix, harmonic by harmonic, from a finite element representation of a general axisymmetric elastic shell. SABOR IV uses a meridionally-curved shell element with eight degrees of freedom having strain displacement relationships derived by Novozhilov (13). Axial and tangential displacements are allowed to vary linearly over the element length, while radial displacement is allowed to take on a cubic variation over the element length. Both slope, $w_{,x}$, and displacement compatibility exist at the boundaries between elements. The DYNAL program subsequently uses the mass and stiffness matrices to generate the corresponding frequencies and mode shapes for each harmonic provided by SABOR IV (n=2 and n=3 are the harmonics which were investigated). Since both programs

are extensively documented in references (14) and (15), they have only been briefly described here.

The shell geometry parameters, circumferential wave numbers, and axial half-wave numbers investigated with SABOR IV-DYNAL were:

$L/a = 20, 15, 10, 5, 3,$ and 1

$a/h = 30$

$n = 2$ and 3

$m = 1, 2, 3, 4,$ and 5

The number of axial half-waves obtained accurately depended upon the number of elements used in our model. For each L/a ratio, two finite element models were used in order to determine the effect of element length on accuracy of results. First four and then eight cylindrical elements were used. Comparing the four and eight element models, differences in the predicted natural frequencies indicated an increase in accuracy as element length was decreased. While the difference for long shells, $L/a \geq 10$ were large, the differences for short shells, $L/a \leq 5$, were small and, therefore, the eight element model was chosen as being satisfactory for this investigation. Models containing additional elements, which would have improved the accuracy for long shells, were not used due to limitations on computer time.

The program's output consisted of frequency in hertz and normalized mode shapes. The mode shapes were used to identify the different axial modes and to locate the nodes for the experimental work.

IV. RESULTS

The preceding paragraphs have described two methods, experimental and finite element, used to check the energy solution, Eqs. (9), (11), and (12), developed in this investigation of free-free cylinders. In the following paragraphs, a comparison of results obtained by the three different methods is presented in terms of a frequency comparison, Table I, and a mode shape comparison, Figs. 6, 7, and 8. Finally, a discussion of results is presented which explains the agreement of results shown in Table I and Figs. 6, 7, and 8.

A. Frequency Comparison

Table I presents natural frequencies obtained by each of the three methods used: energy, experimental, and finite element. These frequencies correspond to the predominately radial modes of vibration. Frequency data are in hertz for easy comparison. In calculating these frequencies, the material properties assumed for the steel cylinders are: Poisson's ratio, $\nu=0.3$; elastic modulus, $E=30{,}000$ ksi; and mass density, $\rho=0.283$ lbs/in^3. To facilitate application of results to cylinders with other material properties, the non-dimensional frequency factor, ω/ω_o, which does not depend on the values of E and ρ, is also presented for the energy solution. Percent deviations between the energy method results and both experimental

Table I. Frequency comparison for free-free cylinders investigated, a/h=30.

MODAL NUMBERS		METHOD OF SOLUTION				PERCENT DEVIATION		NODAL NUMBERS		METHOD OF SOLUTION				PERCENT DEVIATION	
		Energy Method		Experimental	Finite Element					Energy Method		Experimental	Finite Element		
n	m	frequency factor	(freq. hz) ①	(freq. hz) ②	(freq. hz) ③	$=100\cdot\frac{②-①}{①}$	$=100\cdot\frac{③-①}{①}$	n	m	frequency factor	(freq. hz) ①	(freq. hz) ②	(freq. hz) ③	$=100\cdot\frac{②-①}{①}$	$=100\cdot\frac{③-①}{①}$
				L/a = 20								L/a = 5			
2	1	0.0288	495.1	*	558.9	-	+12.9	2	1	0.1734	2974.3	**	2977.6	-	+0.1
"	2	0.0423	725.8	*	1003.6	-	+38.3	"	2	0.3773	6471.1	**	6359.5	-	-1.7
"	3	0.0678	1162.6	1130	1770.3	-2.8	+52.2	"	3	0.5528	9480.3	**	9498.2	-	+0.2
"	4	0.1020	1749.6	*	2801.7	-	+60.0	"	4	0.6760	11,593.6	**	11,831.8	-	+2.1
"	5	0.1421	2437.6	**	4001.8	-	+64.2	"	5	0.7593	13,022.1	**	13,456.7	-	+3.3
3	1	0.0733	1257.9	*	1280.1	-	+1.7	3	1	0.1207	2069.6	2118	2117.5	+2.3	+2.3
"	2	0.0757	1298.7	*	1435.6	-	+10.5	"	2	0.2357	4043.0	**	4218.3	-	+4.3
"	3	0.0812	1392.8	1500	1791.3	+7.7	+28.6	"	3	0.3731	6398.3	**	6834.3	-	+6.8
"	4	0.0912	1565.0	*	2375.2	-	+51.7	"	4	0.5001	8577.2	**	9310.4	-	+8.5
"	5	0.1064	1825.5	1875	3156.9	+2.7	+73.0	"	5	0.6062	10,397.2	**	11,313.4	-	+8.8
				L/a = 15								L/a = 3			
2	1	0.0341	585.5	590	657.6	+0.8	+12.3	2	1	0.3888	6668.3	**	6465.2	-	-3.0
"	2	0.0633	1085.8	*	1363.6	-	+25.6	"	2	0.6692	11,476.5	**	10,746.6	-	-6.4
"	3	0.1093	1875.7	1780	2485.6	-5.1	+32.5	"	3	0.8054	13,812.2	**	13,534.4	-	-2.0
"	4	0.1655	2838.2	**	3902.1	-	+37.5	"	4	0.8841	15,163.0	**	15,147.7	-	-0.0
"	5	0.2267	3888.4	**	5425.0	-	+39.5	"	5	0.9495	16,285.7	**	16,553.2	-	+1.6
3	1	0.0744	1275.4	1345	1301.9	+5.5	+2.1	3	1	0.2421	4151.7	**	4123.5	-	-0.7
"	2	0.0802	1376.9	*	1543.6	-	+12.1	"	2	0.4726	8224.7	**	8006.2	-	-2.6
"	3	0.0938	1609.6	1680	2088.6	+4.3	+29.8	"	3	0.6612	11,340.7	**	11,292.4	-	-0.4
"	4	0.1166	1999.7	1985	2946.7	-0.7	+47.3	"	4	0.7876	13,508.3	**	13,717.1	-	+1.5
"	5	0.1472	2525.4	**	4024.2	-	+59.5	"	5	0.8888	15,244.0	**	15,669.7	-	+2.8
				L/a = 10								L/a = 1			
2	1	0.0547	938.0	940	1011.3	+0.0	+7.8	2	1	0.9349	16,034.2	**	15,459.1	-	-3.6
"	2	0.1245	2136.6	2035	2381.0	-4.7	+11.4	"	2	1.1361	19,485.2	**	19,348.8	-	-0.7
"	3	0.2153	3693.2	**	4245.6	-	+14.9	"	3	1.5308	26,253.1	**	26,227.1	-	-0.1
"	4	0.3119	5349.3	**	6288.5	-	+17.5	"	4	2.1720	37,251.1	**	37,450.1	-	+0.5
"	5	0.4045	6937.4	**	8170.7	-	+17.8	"	5	3.0449	52,222.2	**	52,810.3	-	+1.1
3	1	0.0786	1348.2	1395	1386.1	+3.5	+2.8	3	1	0.8516	14,605.0	**	14,057.9	-	-3.8
"	2	0.0996	1709.1	1765	1928.3	+3.3	+12.8	"	2	1.1378	19,514.2	**	19,007.7	-	-2.6
"	3	0.1407	2413.0	**	2990.5	-	+23.9	"	3	1.5635	26,814.3	**	26,764.0	-	-0.2
"	4	0.1963	3367.2	**	4432.5	-	+31.6	"	4	2.2173	38,027.8	**	38,225.4	-	+0.5
"	5	0.2596	4451.7	**	5997.7	-	+34.8	"	5	3.0950	53,080.8	**	53,668.4	-	+1.9

* Nodal locations were not within the range of test fixture.
** Frequency was not within the range of vibration exciter.

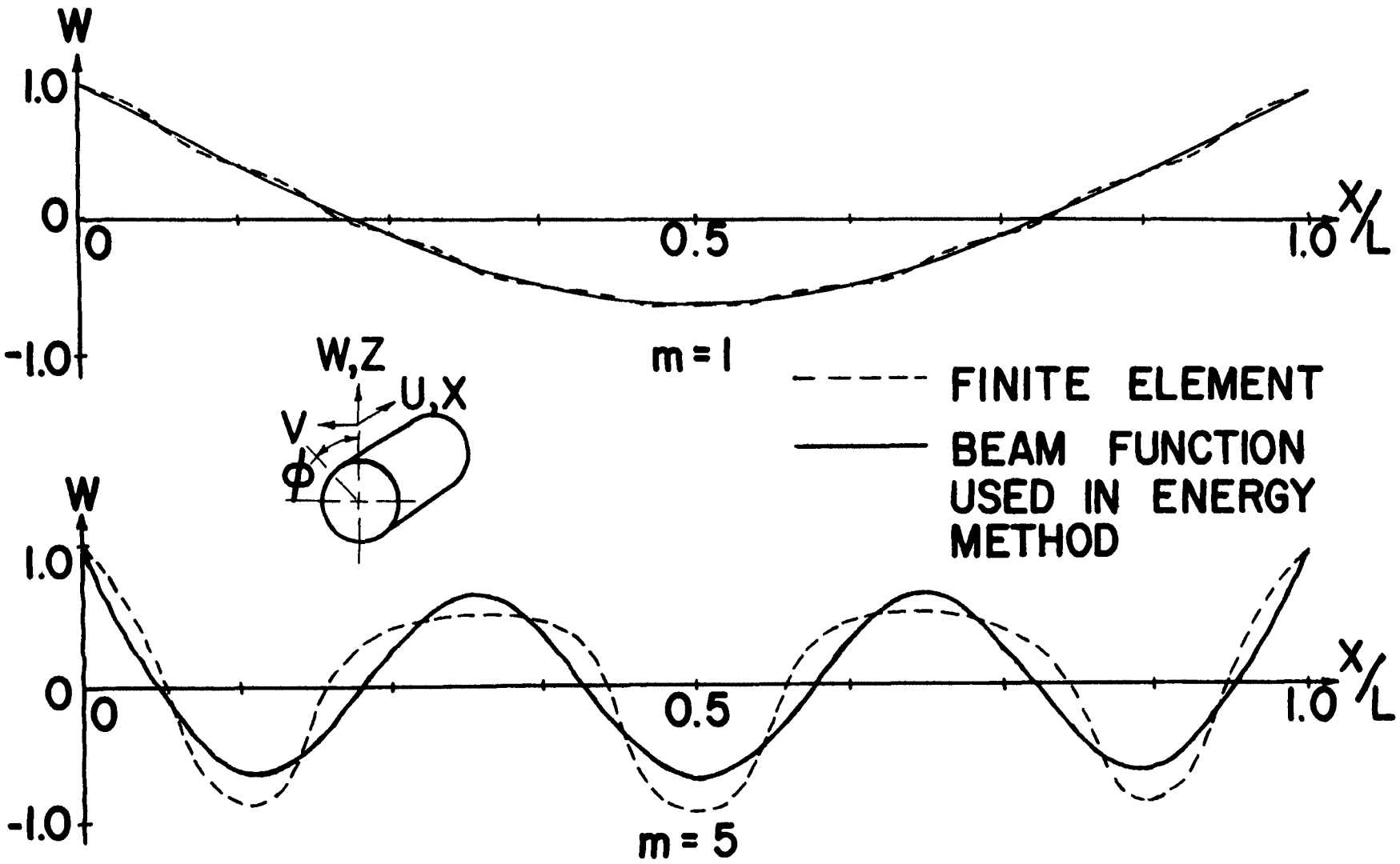

Fig. 6. Mode shape comparison, radial motion component, L/a = 20

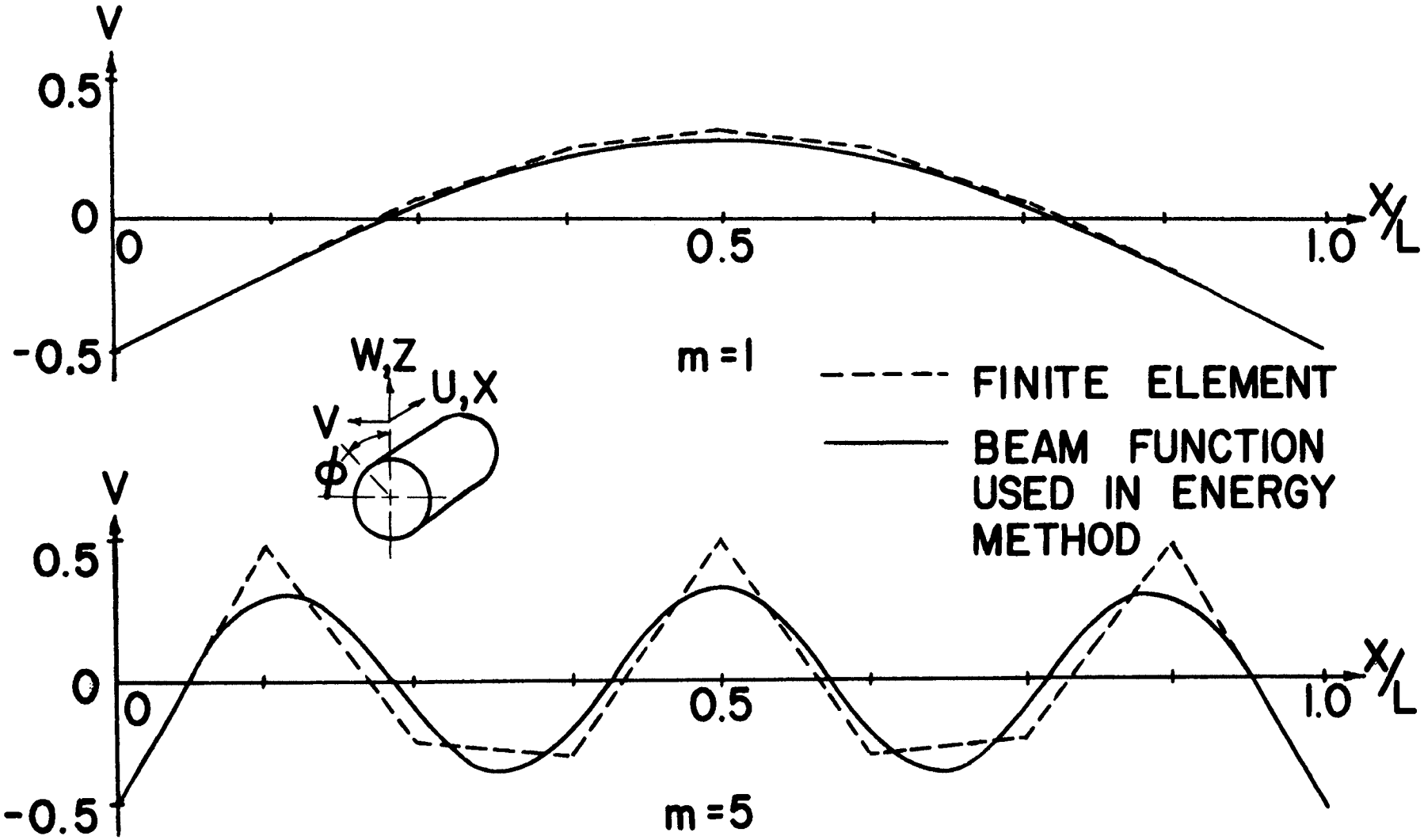

Fig. 7. Mode shape comparison, tangential motion component, L/a = 20

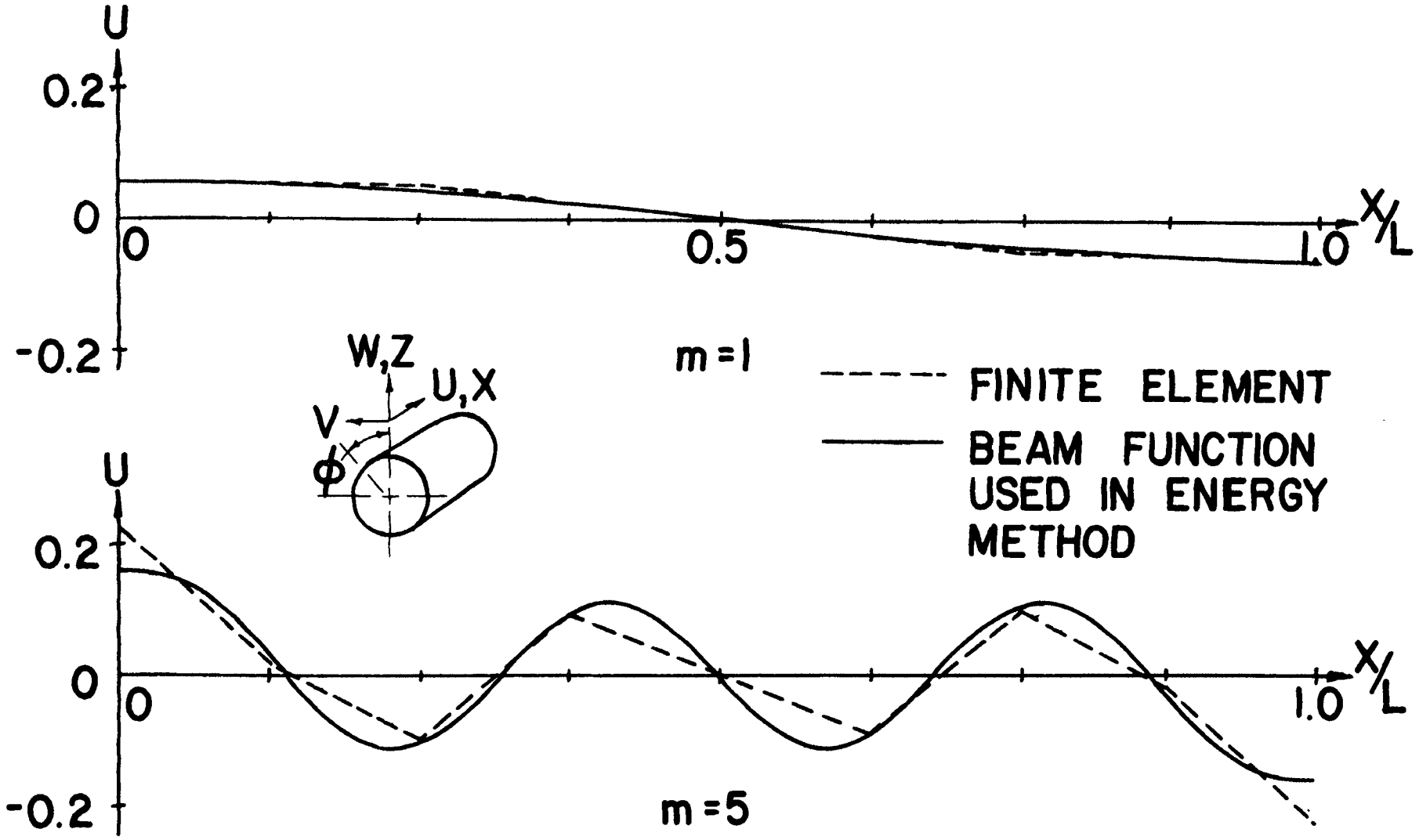

Fig. 8. Mode shape comparison, axial motion component, L/a = 20

and finite element results are presented. Experimental results are not presented for all combinations of modal numbers, n and m, and the geometric parameter, L/a, due to the limitations noted at the bottom of the table.

The experimental natural frequencies deviate by less than eight percent from the corresponding energy method frequencies. Finite element deviations are seen to increase with increasing element-length/radius ratio and increasing axial half-wave number, m. Since eight finite elements were used for all L/a ratios, increasing L/a ratios in Table I signify increasing element-length/radius ratios. For element-length/radius ratios ≤ 0.625 ($L/a \leq 5$) and $m \leq 5$, the deviations of the finite element results from those of the energy method are always less than nine percent. For element-length/radius ratios > 0.625 ($L/a > 5$), the deviations continue to increase with increasing element-length/radius ratio. Much smaller deviations would be expected for $L/a > 5$ if a larger number of finite elements had been used. Due to the increased computer time required for an increased number of finite elements, the finite element results of Table I were all obtained with an eight element model.

B. Mode Shape Comparison

Typical mode shapes from the finite element method and the energy solution are shown in Figs. 6, 7, and 8. Mode shapes shown are predominately radial with L/a=20

and n=2. The radial motion component of mode shape is shown in Fig. 6, the tangential motion component in Fig. 7, and the axial motion component in Fig. 8. As previously noted, the finite element program allows a linear variation of u and v over an element length, while it allows a cubic variation of w over an element length. In presenting the finite element results of Figs. 6, 7, and 8, the normalized mode shape data obtained from the computer output are plotted as points at the stations between finite elements. These points are then connected with a dash line representing the particular variation over an element length which applies. The solid lines of Figs. 6, 7, and 8 are obtained from the assumed beam function displacements used in the energy method. These functions are normalized to C=1 which establishes numerical values for A and B given by the amplitude ratios described in Appendix B.

Visual inspection of the mode shapes of Figs. 6, 7, and 8 gives the following results. The finite element mode shape representation becomes progressively rougher and more approximate as the axial half-wave number, m, increases. This trend was found to be most pronounced for long cylinders (L/a=20) represented in the figures and could be anticipated by checking the frequency results, since the largest finite element frequency deviations occurred for L/a=20 and m=5. Even for this worst case, the agreement between finite element and energy solution mode shapes

is remarkably good.

C. Discussion of Results

The frequency comparison of Table I indicates excellent agreement between the energy method results and those obtained by both methods of verification. An explanation for this agreement shall now be discussed.

For a shell, the four conditions characterizing a free end are

$$N_x=0 \qquad M_x=0 \qquad T_x=0 \qquad S_x=0$$

When the displacement functions of Eqs. (4) and (10) are assumed and the four stress resultants on the x face, N_x, M_x, T_x, and S_x, are evaluated at the boundaries, the stress resultants are found not to vanish. Thus, the assumed displacement forms of Eqs. (4) and (10) do not satisfy the natural boundary conditions of a free-free cylinder. Then why does the energy method of this investigation predict natural frequencies with good accuracy?

The answer to the above question is drawn from Figs. 6, 7, and 8. In these figures, the nodal locations and the modal forms of the assumed displacement functions correspond well with those determined from the finite element method. It is this agreement of radial, tangential, and axial motion mode shapes that has allowed the energy method to predict natural frequencies with good accuracy. If the natural boundary conditions had also been satisfied, the approximate natural frequency of the energy method

would be an upper bound to the exact value of natural frequency for the particular mode (16). However, due to the accuracy indicated by Table I, the fact that the approximate frequencies may not be interpreted as an upper bound makes the results of the energy method of this investigation of no less practical importance. Finally, a more sophisticated form of the Rayleigh-Ritz method could be used to obtain better approximations to the natural frequencies, but again due to the accuracy noted in Table I, further refinement is considered unjustified for most engineering applications.

V. CONCLUSIONS

The energy solution developed in this investigation gives excellent approximations to the natural frequencies of free-free thin cylinders. Furthermore, with only slight modifications, the developed frequency equation for the free-free case is shown to agree with the frequency equations developed by Arnold and Warburton for the fixed-fixed and simply-supported cases. When compared with experimental and finite element results, the maximum deviation of energy method frequencies for the free-free cylinders investigated is less than ten percent. Arnold and Warburton, as well as Sharma, found similar deviations for the fixed-fixed and simply-supported cases.

Excellent agreement also exists between the assumed displacement forms of the energy method and those predicted by the SABOR IV-DYNAL finite element program for the free-free cylinders of this investigation. This agreement has allowed the natural frequencies to be predicted with good accuracy.

BIBLIOGRAPHY

1. Arnold, R. N., and Warburton, G. B., "Flexural Vibrations of Thin Cylinders," Institution of Mech. Engr. Proc., Vol 167, 1953, pp. 62-80.

2. Rayleigh, T. W. S., The Theory of Sound, Dover Publications, Inc., New York, 1894, 2nd ed., Vol. 1, pp. 395.

3. Love, A. E. H., The Mathematical Theory of Elasticity, Cambridge University Press, Cambridge, 1934, 4th ed., pp. 521, 529, 543-549.

4. Flugge, W., Statik und Dynamik der Schalen, Julius Springer-Verlog, Berlin, 1934, pp. 227-232.

5. Arnold, R. N. and Warburton, G. B., "Flexural Vibrations of the Walls of Thin Cylindrical Shells Having Freely-Supported Ends," Proc. Roy. Soc., London, A 197, 1949, pp. 238-256.

6. Flugge, W., Stresses in Shells, Springer-Verlog, Berlin, Hudleberg, New York, 1967, 4th ed., pp. 208-234.

7. Forsberg, K., "Influence of Boundary Conditions on the Modal Characteristics of Thin Cylindrical Shells," AIAA Journal, Vol. 2, No. 12, Dec. 1964, pp. 2150-2157.

8. Sharma, S.K., "Free Vibration of Circular Cylindrical Shells," M.S. Thesis at University of Missouri-Rolla, 1971.

9. Weingarten, V. I. "Free Vibration of Thin Cylindrical Shells," AIAA Journal, Vol. 2, No. 4, Apr. 1964, pp. 717-722.

10. Gottenberg, W. G., "Experimental Study of the Vibrations of a Circular Cylindrical Shell," Journal of the Acoustical Society of America, Vol. 32, No. 8, Aug. 1960, pp. 1002-1006.

11. Forsberg, K., "Axisymmetric and Beam Type Vibrations of Thin Cylindrical Shells," AIAA Journal, Vol. 7, No. 2, Feb. 1969, pp. 221-227.

12. Timoshenko, S., and Woinowski-Krieger, S., Theory of Plates and Shells, McGraw-Hill, New York, 1959, 2nd ed., pp. 430.

13. Novozhilov, V. V., Theory of Thin Shells, P. Noordhoff, Ltd., Groninger, The Netherlands, 1959.

14. Witmer, A. E., Pian, T. H., Mack, E. W., and Berg, B. A., "An Improved Discrete-Element Analysis and Program for the Linear-Elastic Static Analysis of Meridionally-Curved, Variable-Thickness, Branched Thin Shells of Revolution Subjected to General External Mechanical and Thermal Loads," Mass. Inst. of Tech., ASRL RT 1464, Part 1, March, 1968.

15. ICES-DYNAL User Manual, McDonnell Douglas Automation Report, MDC-N0040-021, 1971.

16. Meirovitch, L., Analytical Methods in Vibrations, MacMillan Co., London, 1967, pp. 211-227.

VITA

Dale Elmer Leanhardt was born February 6, 1947, in St. Louis, Missouri. He graduated from Mehlville Senior High School, St. Louis, Missouri, in June 1965. He worked as a co-op for the McDonnell-Douglas Corp., St. Louis, Missouri, while receiving his undergraduate education at the University of Missouri-Rolla, Missouri, and has held the Mehlville PTA Scholarship, 1965-66, and the Murphy Company Freshman Scholarship for Mechanical Engineers, 1965-67. He received a Bachelor of Science degree in Mechanical Engineering from the University of Missouri-Rolla in May, 1970.

He has been enrolled in the Graduate School of the University of Missouri-Rolla, since January 1970 and has held an NSF Fellowship for the period September, 1970, to August, 1971.

APPENDICES

APPENDIX A

INTEGRATIONS FOR STRAIN ENERGY AND KINETIC ENERGY

1. Strain Energy (even number of axial nodes)

$$S = \frac{E}{2(1-\nu^2)} \int_0^{2\pi} \int_{-L/2}^{L/2} \int_{-h/2}^{h/2} \left[e_x^2 + e_y^2 + 2\nu e_x e_y + \tfrac{1}{2}(1-\nu) e_{xy}^2 \right] a \, d\Phi \, dx \, dz \qquad \text{(A-1)}$$

let $$S_1 = \int \int \int e_x^2 \, d\Phi \, dx \, dz \qquad \text{(A-2a)}$$

$$S_2 = \int \int \int e_y^2 \, d\Phi \, dx \, dz \qquad \text{(A-2b)}$$

$$S_3 = 2\nu \int \int \int e_x e_y \, d\Phi \, dx \, dz \qquad \text{(A-2c)}$$

$$S_4 = \tfrac{1}{2}(1-\nu) \int \int \int e_{xy}^2 \, d\Phi \, dx \, dz \qquad \text{(A-2d)}$$

then $$S = \frac{Ea}{2(1-\nu^2)} (S_1+S_2+S_3+S_4) \qquad \text{(A-3)}$$

(a) The integration of Eq. (A-2a) follows.

$$S_1 = (1/a^4) \int_0^{2\pi} \int_{-L/2}^{L/2} \int_{-h/2}^{h/2} \cos^2(n\Phi) \left[(\mu^4 W^2) z^2 - (2aUW\mu^3) z + \mu^2 a^2 U^2 \right] \left(\cos^2 \frac{\mu}{a} x + 2k \cos \frac{\mu}{a} x \cosh \frac{\mu}{a} x + k^2 \cosh^2 \frac{\mu}{a} x \right) d\phi \, dx \, dz$$

Carrying out this integration in three parts, the integrations are

$$\int_{-h/2}^{h/2} F(z) \, dz = ha^2(\mu^4 W^2 \beta + \mu^2 U^2) \qquad \text{(A-4a)}$$

$$\int_0^{2\pi} G(\Phi)\, d\Phi = \pi \qquad \text{(A-4b)}$$

$$\int_{-L/2}^{L/2} H(x)\, dx = \frac{L}{2}(1+k^2) + \frac{\sin\frac{\mu}{a}L}{2\frac{\mu}{a}} + k^2 \frac{\sinh\frac{\mu}{a}L}{2\frac{\mu}{a}}$$

$$+ \frac{\sin\frac{\mu}{a}L}{\frac{\mu}{a}} + k^2 \frac{\sinh\frac{\mu}{a}L}{\frac{\mu}{a}} \qquad \text{(A-4c)}$$

The results of the integration over x can be further simplified by evaluating k^2, which becomes after using the relationships, $\tan\frac{\mu L}{2a} = -\tanh\frac{\mu L}{2a}$ and $k = \sin\frac{\mu L}{2a}/\sinh\frac{\mu L}{2a}$:

$$k^2 = -\frac{\sin\frac{\mu}{a}L}{\sinh\frac{\mu}{a}L} \qquad \text{(A-5)}$$

Substituting Eq. (A-5) into Eq. (A-4c), the integration over x becomes

$$\int_{-L/2}^{L/2} H(x)\, dx = \frac{L}{2}(1+k^2) = \frac{L}{2}\Theta_1$$

and S_1 becomes

$$S_1 = \frac{\pi h L}{2a^2}(\Theta_1\mu^4 W^2\beta + \Theta_1\mu^2 U^2)$$

where $\beta = \frac{h^2}{12a^2}$

$$\Theta_1 = (1+k^2)$$

(b) The integration of Eq. (A-2b) follows.

$$S_2 = (1/a^4) \int_0^{2\pi} \int_{-L/2}^{L/2} \int_{-h/2}^{h/2} \cos^2(n\Phi)$$

$$\left[a^2(Vn-W)^2 - 2a(Vn-W)(nV-n^2W)z + (nV-n^2W)^2z^2\right]$$

$$(\cos^2\tfrac{\mu}{a}x - 2k\cos\tfrac{\mu}{a}x\cosh\tfrac{\mu}{a}x + k^2\cosh^2\tfrac{\mu}{a}x)\, d\Phi\, dx\, dz$$

Carrying out this integration in three parts, the integrations are

$$\int_{-h/2}^{h/2} F(z)\, dz = a^2h\left[(Vn-W)^2 + (nV-n^2W)^2\beta\right]$$

$$\int_0^{2\pi} G(\Phi)\, d\Phi = \pi$$

$$\int_{-L/2}^{L/2} H(x)\, dx = \frac{L}{2}\Theta_1 \text{ (integration similar as for } S_1)$$

and S_2 becomes

$$S_2 = \frac{\pi hL}{2a^2}\Theta_1\left[(Vn-W)^2 + (nV-n^2W)^2\beta\right]$$

(c) The integration of Eq. (A-2c) follows.

$$S_3 = \frac{2\nu}{a^4}\int_0^{2\pi}\int_{-L/2}^{L/2}\int_{-h/2}^{h/2}\cos^2(n\Phi)$$

$$\{[W\mu^2a(Vn-W) + \mu aU(nV-n^2W)]z - [W\mu^2(nV-n^2W)]z^2$$

$$- [\mu a^2U(Vn-W)]\}\,(\cos^2\tfrac{\mu}{a}x - k^2\cosh^2\tfrac{\mu}{a}x)\, d\Phi\, dx\, dz$$

Carrying out this integration in three parts, the integrations are

$$\int_{-h/2}^{h/2} F(z)\, dz = ha^2\left[-\mu nUV + \mu UW + \beta(\mu^2n^2W^2 - n\mu^2VW)\right]$$

$$\int_0^{2\pi} G(\Phi)\, d\Phi = \pi$$

$$\int_{-L/2}^{L/2} H(x)\, dx = \frac{\sin\frac{\mu}{a}L}{2\frac{\mu}{a}} + \frac{L}{2} - k^2 \frac{\sinh\frac{\mu}{a}L}{2\frac{\mu}{a}} - k^2\left(\frac{L}{2}\right)$$

Substituting k^2 from Eq. (A-5)

$$\int_{-L/2}^{L/2} H(x)\, dx = \frac{L}{2}\left[(1-k^2) + \frac{2a}{\mu L}\sin\frac{\mu}{a}L\right] = \frac{L}{2}\,\Theta_2$$

and S_3 becomes

$$S_3 = \frac{\nu h \pi L}{a^2}\,\Theta_2\left[\mu UW - \mu nUV + \beta(\mu^2 n^2 W^2 - n\mu^2 WV)\right]$$

(d) The integration of Eq. (A-2d) follows.

$$S_4 = \frac{(1-\nu)}{2a^4}\int_0^{2\pi}\int_{-L/2}^{L/2}\int_{-h/2}^{h/2} \sin^2(n\Phi)$$

$$\{[a^2(\mu V - nU)^2] - [2\mu a(\mu V - nU)(V - nW)]z$$

$$+ [4\mu^2(V-nW)^2]\, z^2\}\,(\sin^2\tfrac{\mu}{a}x + 2k\sin\tfrac{\mu}{a}x\sinh\tfrac{\mu}{a}x$$

$$+ k^2\sinh^2\tfrac{\mu}{a}x)\, d\Phi\, dx\, dz$$

Carrying out this integration in three parts, the integrations are

$$\int_{-h/2}^{h/2} F(z)\, dz = a^2 h\left[(n^2U^2 + \mu^2V^2 - 2\mu nUV)\right.$$

$$\left. + 4\beta(\mu^2V^2 + \mu^2n^2W^2 - 2\mu^2 nVW)\right]$$

$$\int_0^{2\pi} G(\Phi)\, d\Phi = \pi$$

$$\int_{-L/2}^{L/2} H(x)\, dx = (1-k^2)\frac{L}{2} + 3k^2\frac{\sinh\frac{\mu}{a}L}{2\frac{\mu}{a}} - 3\frac{\sin\frac{\mu}{a}L}{2\frac{\mu}{a}}$$

Substituting k^2 from Eq. (A-5)

$$\int_{-L/2}^{L/2} H(x)\,dx = \frac{L}{2}\left[(1-k^2) - \frac{6a}{\mu L}\sin\frac{\mu}{a}L\right] = \frac{L}{2}\,\Theta_3$$

and S_4 becomes

$$S_4 = \frac{\frac{1}{2}(1-\nu)h\pi L}{2a^2}\,\Theta_3\left[(n^2U^2 + \mu^2V^2 - 2\mu nUV)\right.$$

$$\left. + 4\beta(\mu^2V^2 + \mu^2n^2W^2 - 2\mu^2nVW)\right]$$

(e) Finally, substituting the results for S_1, S_2, S_3, and S_4 back into Eq. (A-3), the expression for strain energy given in the body of the thesis, Eq. (5) is obtained.

2. Kinetic Energy (even number of axial nodes)

$$T = \frac{\rho}{2g}\int_0^{2\pi}\int_{-L/2}^{L/2}\int_{-h/2}^{h/2}\left[(u,_t)^2 + (v,_t)^2 + (w,_t)^2\right]$$

$$a\,d\Phi\,dx\,dz \qquad \text{(A-6)}$$

let $T_1 = \int\int\int (u,_t)^2\,d\Phi\,dx\,dz$ (A-7a)

$$T_2 = \int\int\int (v,_t)^2\,d\Phi\,dx\,dz \qquad \text{(A-7b)}$$

$$T_3 = \int\int\int (w,_t)^2\,d\Phi\,dx\,dz \qquad \text{(A-7c)}$$

then $T = \frac{\rho a}{2g}(T_1+T_2+T_3)$ (A-8)

(a) The integration of Eq. (A-7a) follows.

$$T_1 = \int_0^{2\pi}\int_{-L/2}^{L/2}\int_{-h/2}^{h/2}\dot{U}^2(\sin^2\frac{\mu}{a}x + 2k\sin\frac{\mu}{a}x\sinh\frac{\mu}{a}x$$

$$+ k^2\sinh^2\frac{\mu}{a}x)\cos^2(n\Phi)\,d\Phi\,dx\,dz$$

The integrations take the same form as section (1d); the results are

$$T_1 = \frac{\pi L h}{2} \Theta_3 \dot{U}^2$$

(b) The integration of Eq. (A-7b) follows.

$$T_2 = \int_0^{2\pi} \int_{-L/2}^{L/2} \int_{-h/2}^{h/2} \dot{V}^2 (\cos^2 \frac{\mu}{a} x - 2k \cos \frac{\mu}{a} x \cosh \frac{\mu}{a} x + k^2 \cosh^2 \frac{\mu}{a} x) \sin^2 (n\Phi) \, d\Phi \, dx \, dz$$

The integration takes the same form as section (1b); the results are

$$T_2 = \frac{\pi L h}{2} \Theta_1 \dot{V}^2$$

(c) The integration of Eq. (A-7c) follows.

$$T_3 = \int_0^{2\pi} \int_{-L/2}^{L/2} \int_{-h/2}^{h/2} \dot{W}^2 (\cos^2 \frac{\mu}{a} x - 2k \cos \frac{\mu}{a} x \cosh \frac{\mu}{a} x + k^2 \cosh^2 \frac{\mu}{a} x) \sin^2 (n\Phi) \, d\Phi \, dx \, dz$$

The integrations are identical with those of T_2; the results are

$$T_3 = \frac{\pi L h}{2} \Theta_1 \dot{W}^2$$

(d) Finally, substituting the results for T_1, T_2, and T_3 back into Eq. (A-8), the expression for kinetic energy given in the body of the thesis, Eq. (6), is obtained.

3. The integrations for strain energy and kinetic energy follow a similar form for the case of an odd number of axial nodes.

APPENDIX B

REDUCTION TO FREQUENCY EQUATION AND AMPLITUDE RATIOS

1. The three equations of motion obtained from Lagrange's equation are

$$\{\mu^2\Theta_1 + \tfrac{1}{2}(1-\nu)n^2\Theta_3 - \Delta\Theta_3\}A - \{\tfrac{1}{2}(1-\nu)\mu n\Theta_3 + \nu\mu n\Theta_2\}B + \{\nu\mu\Theta_2\}C = 0$$

$$-\{\nu\mu n\Theta_2 + \tfrac{1}{2}(1-\nu)\Theta_3\mu n\}A + \{n^2\Theta_1 + \tfrac{1}{2}(1-\nu)\mu^2\Theta_3 - \Delta\Theta_1 + \beta[n^2\Theta_1 + 2(1-\nu)\mu^2\Theta_3]\}B - \{n\Theta_1 + \beta[n^3\Theta_1 + \nu\mu^2 n\Theta_2 + 2(1-\nu)\mu^2 n\Theta_3]\}C = 0$$

$$\{\nu\mu\Theta_2\}A - \{n\Theta_1 + \beta[n^3\Theta_1 + \nu\mu^2 n\Theta_2 + 2(1-\nu)\mu^2 n\Theta_3]\}B + \{\Theta_1 - \Delta\Theta_1 + \beta[\mu^4\Theta_1 + n^4\Theta_1 + 2\nu\mu^2 n^2\Theta_2 + 2(1-\nu)\mu^2 n^2\Theta_3]\}C = 0$$

2. Reduction process

The above system of equations are of the form

$$x_1A + y_1B + z_1C = 0 \qquad \text{(B-1a)}$$

$$x_2A + y_2B + z_2C = 0 \qquad \text{(B-1b)}$$

$$x_3A + y_3B + z_3C = 0 \qquad \text{(B-1c)}$$

where $x_1 = (G-\Delta\Theta_3)$ (B-1d)

$y_2 = (H-\Delta\Theta_1)$ (B-1e)

$z_3 = (J-\Delta\Theta_1)$ (B-1f)

From (B-1a)

$$C = -\frac{1}{z_1}(x_1A + y_1B) \tag{B-2}$$

substituting into (B-1b) and (B-1c)

$$(x_2 - x_1z_2/z_1)A + (y_2 - y_1z_2/z_1)B = 0 \tag{B-3a}$$

$$(x_3 - x_1z_3/z_1)A + (y_3 - y_1z_3/z_1)B = 0 \tag{B-3b}$$

from (B-3b)

$$B = -\frac{(x_3 - x_1z_3/z_1)}{(y_3 - y_1z_3/z_1)}\ A \tag{B-4}$$

substituting into (B-3a), dividing through by A, and simplifying, the results are

$$(x_2y_3z_1 - x_1y_3z_2 - x_2y_1z_3) - (x_3y_2z_1 - x_3y_1z_2 - x_1y_2z_3) = 0 \tag{B-5}$$

substituting x_1, y_2, and z_3 from Eqs. (B-1d), (B-1e), and (B-1f), the desired cubic frequency equation is obtained

$$-(\theta_1^2\theta_3)\Delta^3 + (J\theta_1\theta_3 + H\theta_1\theta_3 + G\theta_1^2)\Delta^2 + (y_3z_2\theta_3 + y_1x_2\theta_1 + x_3z_1\theta_1 - GJ\theta_1 - GH\theta_1 - HJ\theta_3)\Delta + (x_2y_3z_1 - Gy_3z_2 - y_1x_2J - x_3z_1H + x_3y_1z_2 + GHJ) = 0 \tag{B-6}$$

Eq. (B-6) can be arranged in the form of Eq. (9) found in the body of the thesis, as follows

$$\Delta^3 - R_2\Delta^2 + R_1\Delta - R_o = 0 \tag{B-7}$$

where $R = 1/(\Theta_1^2\Theta_3)$

$R_2 = R(J\Theta_1\Theta_3 + H\Theta_1\Theta_3 + G\Theta_1^2)$

$R_1 = R(GJ\Theta_1 + GH\Theta_1 - HJ\Theta_3 - y_3z_2\Theta_3 - y_1x_2\Theta_1 - x_3z_1\Theta_1)$

$R_0 = R(x_2y_3z_1 - Gy_3z_2 - y_1x_2J - x_3z_1H - x_3y_1z_2 + GHJ)$

$G = \left[\mu^2\Theta_1 + \tfrac{1}{2}(1-\nu)n^2\Theta_3\right]$

$H = \{n^2\Theta_1 + \tfrac{1}{2}(1-\nu)\mu^2\Theta_3 + \beta[n^2\Theta_1 + 2(1-\nu)\mu^2\Theta_3]\}$

$J = \{\Theta_1 + \beta[\mu^4\Theta_1 + n^4\Theta_1 + 2\nu\mu^2n^2\Theta_2 + 2(1-\nu)\mu^2n^2\Theta_3]\}$

$y_1 = -\left[\nu\mu n\Theta_2 + \tfrac{1}{2}(1-\nu)\mu n\Theta_3\right]$

$z_1 = \nu\mu\Theta_2$

$z_2 = -\{n\Theta_1 + \beta[n^3\Theta_1 + \nu\mu^2n\Theta_2 + 2(1-\nu)\mu^2n\Theta_3]\}$

$x_2 = y_1$

$y_3 = z_2$

$x_3 = z_1$

$\Delta = \rho a^2\omega^2(1-\nu^2)/Eg$

Solving the cubic frequency equation, Eq. (B-7), for the three roots Δ_1, Δ_2, and Δ_3, frequency in radians per second is obtained from

$$\omega_i = \frac{1}{a}\sqrt{\frac{\Delta_i Eg}{\rho(1-\nu^2)}} \qquad \text{where } i = 1, 2, \text{ and } 3 \qquad \text{(B-8)}$$

The amplitude ratios among the three displacements u, v, and w can be obtained for each frequency root by applying Eqs. (B-2) and (B-4). Normalizing to A and using the same expressions defined in Eq. (B-7), the results are

$$(B/A)_i = - \frac{\left[x_3 - (G-\Delta_i\Theta_3)(J-\Delta_i\Theta_1)/z_1\right]}{\left[y_3 - y_1(J-\Delta_i\Theta_1)/z_1\right]} \qquad \text{(B-9a)}$$

$$(C/A)_i = -\frac{1}{z_1} \left\{x_1 - y_1 \frac{\left[x_3 - (G-\Delta_i\Theta_3)(J-\Delta_i\Theta_1)/z_1\right]}{\left[y_3 - y_1(J-\Delta_i\Theta_1)/z_1\right]}\right\} \qquad \text{(B-9b)}$$